Journal of Inclusion Phenomena and Macrocyclic Chemistry **49**: 27–32, 2004.

Modulating Electron Transfer in a Simple Bichromophoric System Employing Axial-Ligation as an Organising Precept

KENNETH P. GHIGGINO[1], JAMES A. HUTCHISON[1], STEVEN J. LANGFORD[2*], MARCIA A.-P. LEE[2], PHILIP R. LOWENSTERN[1] and TREVOR YANN[2]
[1]*School of Chemistry, University of Melbourne, Victoria 3010, Australia;* [2]*School of Chemistry and Centre for Green Chemistry, Monash University, Clayton, Victoria 3800, Australia*

(Received: 15 July 2003; in final form: 13 November 2003)

Key words: coordination, distance dependence, electron transfer, ^{1}H NMR spectroscopy, metalloporphyrin, molecular recognition

Abstract

A naphthalene diimide acceptor **1** bearing a pyridine group linked directly (**a** series) or through a —CH_2CH_2— spacer (**b** series) coordinated axially to a metallotetraarylporphyrin (MP) undergoes fast photoinduced electron transfer (in the case of MP = Zn(II)TTP) while the kinetically more stable ruthenium complexes (MP = Ru(CO)TPP) have been used to illustrate the correlation between the distance of probe protons from the porphyrin plane and the change in chemical shift ($\Delta\delta$) upon coordination. Changes in the emission spectra at 650 nm (λ_{ex} = 400 nm) upon the addition of Zn(II) ions and/or **1b** to $TTPH_2$ can be interpreted in a truth table to illustrate a NAND gate.

Introduction

The success of the photosynthetic reaction centre [1] as an energy transduction device depends primarily on the assembly being able to exert strict control over a number of design features, such as the separation and orientation of the various redox centres and the nature of the medium separating them. One approach to construction of viable mimics that reflect either the complexity or mode of action of naturally occuring reaction centres is to use metal ligation as an organising precept [2–6]. In this way, it is possible to utilise different free-base and metalloporphyrins for the fabrication of one, two or three dimensional assemblies with varying redox, spectral and photophysical properties by virtue of the metal centre employed [4, 5]. In order for these goals to be achievable, more has to be learnt about the interplay of molecular components bearing donor and acceptor groups and the appropriate design principles needed for the generation of complex systems. Here, we demonstrate how a simple bichromophoric system **1**·Zn(II)TTP bearing a metalloporphyrin electron donor and a naphthalene diimide electron acceptor [6] can be assembled through metal ligation to undergo photoinduced ET processes [7] and suggest that these ET processes are tunable by varying the nature and length of the bridge between donor and acceptor. Investigations of this type, in which spectroscopic changes are observed between chromophores, may also yield molecular devices outside of the desired energy transduction devices, e.g., molecular logic gates. The nature of the equilibrium mix of $TTPH_2$ and chemical inputs (in this case **1b**, Zn^{2+}) leading to changes in emission wavelength or intensity (spectroscopic outputs) is also discussed.

* Author for correspondence. E-mail: s.langford@sci.monash.edu.au

Experimental

General procedures

Melting points (m.p.) were measured on a Stuart Scientific melting point apparatus. Low-resolution mass spectra were recorded on a Micromass Platform II spectrometer. Samples were ionised using an electrospray ionisation (ESI) source in positive mode and recorded as the solutions specified. ^{1}H and ^{13}C NMR nuclear magnetic resonance (n.m.r.) spectra were recorded using the Brüker 300DPX spectrometer operating at 300 and 75 MHz, respectively, as solutions in the deuterated solvents specified. Chemical shifts (δ) were calibrated against the residual solvent peak.

Absorption spectra were recorded with a Varian Cary 50 Bio UV–visible spectrophotometer using matched quartz cells (10 mm); uncorrected emission spectra were obtained with either a Varian Eclipse spectrophotometer or a Perkin Elmer LS50B luminescence spectrometer

using a quartz fluorimeter cell (10 mm). All spectroscopic experiments were carried out at room temperature and in spectroscopic grade dichloromethane solution and degassed by repeated freeze-pump-thaw cycles. Binding constants were determined by UV–vis titration. Fluorescence decay profiles were collected using the Time-Correlated Single Photon Counting technique. The excitation source was the synchronously mode-locked and cavity dumped output of a dye laser (Spectra Physics 375, Rhodamine 6G). This allowed selective excitation of the porphyrin Q-bands (570–605 nm) over the NDI.

*Synthesis of bis-N,N′-(4-pyridine)-1,4,5,8-naphthalenetetracarboxylic diimide (**1a**)*

4-Aminopyridine (0.56 g, 5.94 mmol) was added to a stirred solution of 1,4,5,8-naphthalenetetracarboxylic dianhydride (0.60 g, 2.22 mmol) in dry DMF (20 mL). The reaction was heated to 90 °C and left to stir overnight. Once complete, the reaction mixture was cooled to room temperature. Water (20 mL) was added and the resulting precipitate collected and air dried to yield **1a** (0.55 g, 59%) as an off-white precipitate. M.p. > 300 °C. Spectroscopic data obtained for **1a** by this method were consistent with the results reported by Miller and coworkers [8]. ^{1}H nmr (300 MHz, d_6-DMSO:aq HCl (3M); 1:1): δ 9.04, d, J 6.34 Hz, 4H, Ar—H; 8.69, s, 4H, Ar—H; 8.26, d, J 6.55 Hz, 4H, Ar—H. Mass spectrum (ESI): m/z 421.1 ($[M + H]^+$).

*Synthesis of bis-N,N′-4-(2-ethyl)pyridine-1,4,5,8-naphthalenetetracarboxylic diimide (**1b**)*

4-(2-Aminoethyl)pyridine [9] **2b** (0.55 g, 4.50 mmol) was added to a stirred solution of 1,4,5,8-naphthalenetetracarboxylic dianhydride (0.50 g, 1.87 mmol) and K_2CO_3 (0.26 g, 1.87 mmol) in dry DMF (50 mL). The reaction was left to stir overnight at room temperature. Once complete, the reaction mixture was filtered and water (20 mL) was added to the filtrate. The resulting precipitate was collected at the pump and air-dried to yield **1b** (0.41 g, 46%) as an off-white solid m.p. > 300 °C. ^{1}H NMR (300 MHz, $CDCl_3$): δ 8.77, s, 4H, Ar—H; 8.55, br, 4H, Ar—H; 7.27, d, J 4.7 Hz, 4H, Ar—H; 4.47, t, J 7.8 Hz, 4H, CH_2; 3.07, t, J 7.8 Hz, 4H, CH_2. ^{13}C NMR (75 MHz, $CDCl_3$): δ 165.9, 152.7, 149.7, 140.1, 131.5, 126.9, 126.3, 41.3, 33.8. Mass spectrum (ESI): m/z 477.1 ($[M + H]^+$).

***1a**.Ru(CO)TPP$_2$*

5,10,15,20-Tetraphenyl 21*H*,23*H*-porphine ruthenium(II) carbonyl (16.7 mg, 0.02 mmol) was added bis-*N,N′*-(4-pyridine)-1,4,5,8-naphthalenetetracarboxylic diimide **1a** (4.7 mg, 0.01 mmol) in based-washed $CDCl_3$ and heated to reflux to overnight. The product was purified by column chromatography (neutral alumina; $CHCl_3$) to obtain the target compound (19.5 mg, 91%) as a purple solid. ^{1}H nmr (300 MHz, $CDCl_3$): δ 8.60, s, 16H, β-pyrollic H; 8.17, d, J 8.4 Hz, 4H, 8.03, d, J 6.2 Hz, 4H,

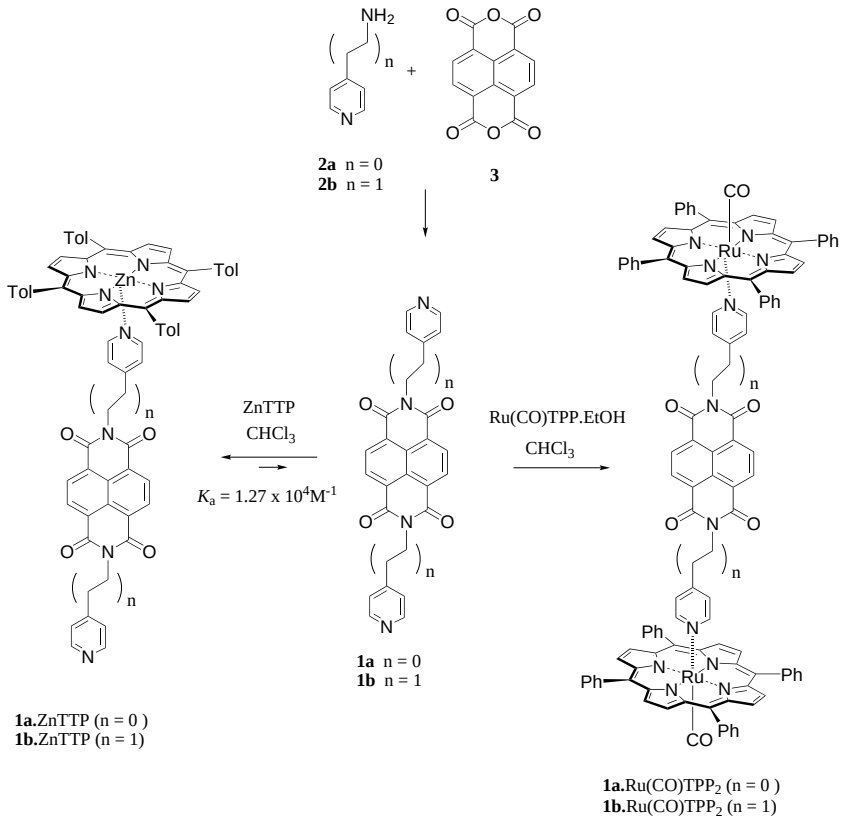

Scheme 1. Reagents and conditions: (a) DMF, K_2CO_3, r.t.; (b) ZnTTP or Ru(CO)TPP, $CDCl_3$.

ArH; 7.69, m, 16H, *meso*-ArH; 7.23, m, 24H, *meso*-ArH; 7.18, d, *J* 7.4 Hz, 16H, *meso*-ArH; 5.15, d, *J* 6.0 Hz, 4H, ArH; 2.35, s, 16H; 1.67, d, *J* 6.9 Hz, 4H, ArH. ^{13}C nmr (75 MHz, $CDCl_3$): δ 163.2, 155.4, 150.6, 140.1, 135.3, 134.5, 133.3, 134.6, 132.4, 127.8, 126.8, 123.6, 109.9. Mass spectrum (ESI): *m*/*z* 421 ([**1a** + H]$^+$), 742 ([Ru(CO)TPP]$^+$), 1162 ([**1a** + Ru(CO)TPP + H]$^+$)

1b. *Ru(CO)TPP*$_2$

5,10,15,20-Tetraphenyl-21*H*,23*H*-porphine ruthenium-(II) carbonyl (14.9 mg, 0.02 mmol) was added bis-*N*,*N*′-4-(2-ethyl)pyridine-1,4,5,8-naphthalenetetracarboxylic diimide **1b** (4.8 mg, 0.01 mmol) in based-washed $CDCl_3$ and heated to reflux to overnight. The product was purified by column chromatography (neutral alumina; $CHCl_3$) to obtain the target compound (14.0 mg, 71%) as a purple solid. ^{1}H nmr (300 MHz, $CDCl_3$): δ 8.57, s, 16H, β-pyrollic H; 8.31, s, 4H, ArH; 8.21, m, 8H, *meso*-ArH; 7.97, m, 16H, *meso*-ArH; 7.71–7.64, m, 24H, *meso*-ArH; 5.16, d, *J* 4.8 Hz, 4H, ArH; 3.42, t, *J* 7.8 Hz, 4H, CH_2; 1.87, t, *J* 7.8 Hz, 4H, CH_2; 1.45, d, *J* 4.8 Hz, 4H, ArH. ^{13}C nmr (75 MHz, $CDCl_3$): δ 162.2, 145.9, 144.2, 143.9, 143.0, 134.6, 134.3, 132.0, 131.2, 127.6, 126.9, 126.6, 126.3, 122.4, 121.9. Mass spectrum (ESI): *m*/*z* 477 ([**1b** + H]$^+$), 742 ([Ru(CO)TPP]$^+$), 1219 ([**1b** + Ru(CO)TPP + H]$^+$).

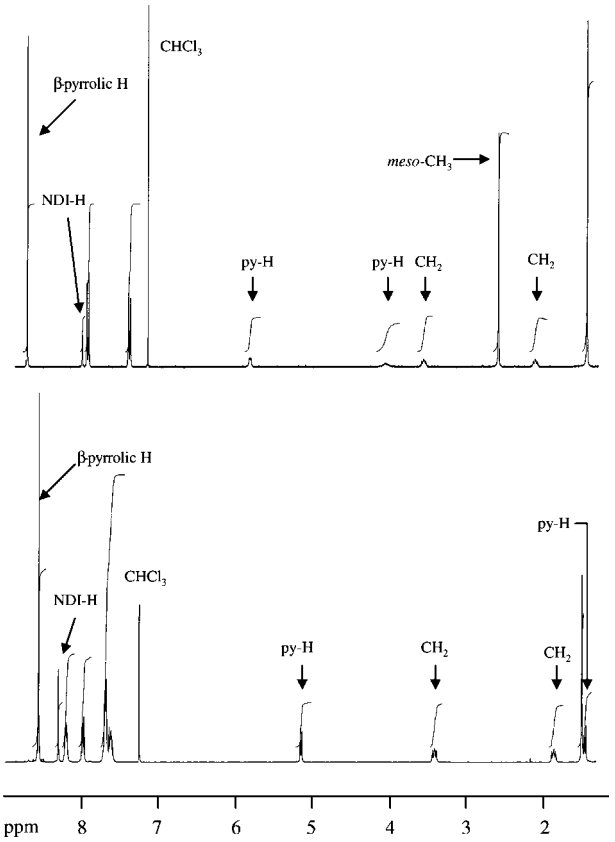

Figure 1. ^{1}H NMR spectrum (300 MHz) at 300 K for a $CDCl_3$ solution of (a) **1b**·Zn(II)TTP_2 and (b) **1b**·Ru(II)(CO)TPP_2. Note the broadening of peaks associated with the diimide unit.

Results

We have chosen to use a naphthalene diimide (NDI) bearing two pyridyl units as the acceptor component of our complex. The reason is twofold. The two pyridyl groups will assure significant formation of the 1:1 complex in solution at concentrations required for ET studies. Secondly, the uncomplexed pyridine may eventually act as a molecular alligator clip for attachment of such complexes to metal surfaces (electrodes). The synthesis of diimides **1a,b** were achieved in 59% (**1a**) [8] and 46% (**1b**) yield by the reaction of two equivalents of 4-aminopyridine (**2a**) (DMF, 90 °C, 12 h) or 4-(ethylamino)pyridine [9] **2b** (DMF, K_2CO_3, r.t., 12 h) with the dianhydride **3** (Scheme 1). We have found that the addition of K_2CO_3 causes an increase in the condensation reaction rate, allowing the use of sensitive or low boiling amines in this reaction. Mixing of **1a** or **1b** with two equivalents of Zn(II)TTP in $CDCl_3$ gave rise to a ^{1}H NMR spectrum in which the resonances associated with the pyridyl groups on the acceptor component were shifted significantly upfield from the chemical shift of the single component in $CDCl_3$ [10]. The slow exchange process between the ZnTTP and five-coordinate Zn(II) complexes, culminating in a proportion of the complexes **1**·$(ZnTTP)_m$ ($m = 0,1$; Scheme 1) being formed, leads to a broadening of NDI signals at room temperature (Figure 1). UV–vis spectra obtained in CH_2Cl_2 solution further support the formation of a complex. Addition of **1a** or **1b** effects a bathochromic shift of the porphyrin absorption, characteristic of axial ligation of Zn(II)TPP by nitrogen donor ligands [11]. Careful titration of **1b** into Zn(II)TTP revealed clean isosbestic points for the absorption shift and allowed the calculation of an association constant (K_a) using standard methods [12]. The K_a was determined as $1.3\times10^4\,M^{-1}$ per Zn(II)TTP–pyridyl interaction for the addition of one porphyrin to the **1b** acceptor. This compares with a K_a of $9.12\times10^3\,M^{-1}$ reported for Zn(II)TPP binding to 4-picoline in CH_2Cl_2 [13]. Job's plot analysis [14] obtained in CH_2Cl_2 at 548 nm for the addition of **1b** to ZnTTP clearly indicates that the formation of the 2:1 Zn(II)TTP:NDI complex is insignificant at porphyrin concentrations ($\approx$10 μM) required for the optically dilute solutions used in photophysical studies. Interestingly, the K_a for **1a**·Zn(II)TTP has been measured as $3.3\times10^3\,M^{-1}$. The smaller value can be attributed to the insolubility of **1a** and its propensity to aggregate as evinced by the presence of some excimer fluorescence.

Replacement of Zn(II)TTP with Ru(CO)TPP, which forms more kinetically stable complexes with pyridines [15, 16], make a useful structural variation to its zinc(II) counterpart. Mixing of **1a** or **1b** with two equivalents of Ru(CO)TPP (60 °C, 3 h) in $CHCl_3$ solution gave rise to highly soluble complexes **1**·$(Ru(CO)TPP)_2$ in 85% (**1a**)

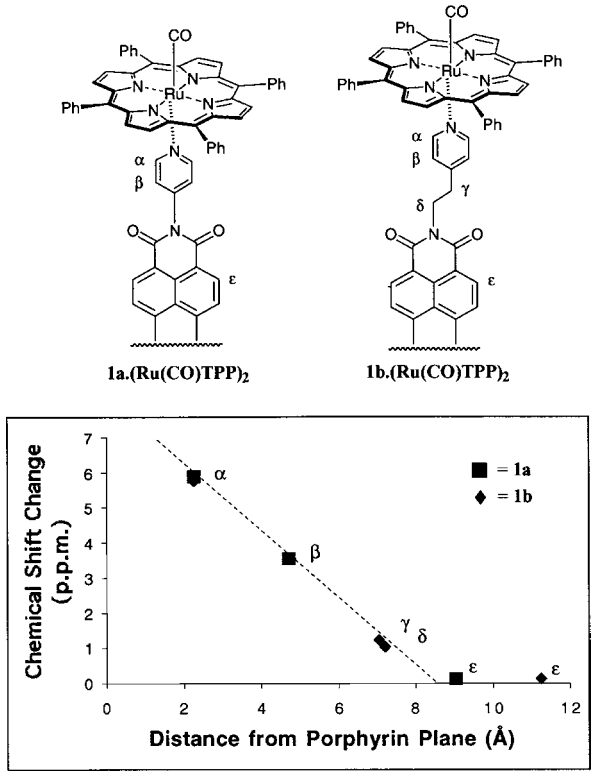

Figure 2. Porphyrin-induced ^{1}H NMR chemical shift changes (at 300 MHz) *versus* the distance from porphyrin plane for **1**·Ru(CO)TPP$_2$ observed at 300 K in $CDCl_3$ solution. In each case, $\Delta\delta = \delta$ (complex) $- \delta$ (free NDI).

and 71% (**1b**) yield after chromatography on neutral alumina. Integration of the ^{1}H NMR spectra readily confirms the stoichiometry of both **1**·(Ru(CO)TPP)$_2$ complexes to be 2:1, consistent with the formation of the trimeric structures (Scheme 1). The influence of the porphyrin ring currents experienced by the protons on the pyridine linker again lead to large chemical shift changes in the ^{1}H NMR spectrum (Figure 1), similar to those obtained for **1a**·(ZnTTP)$_m$ at 243 K. A plot of $\Delta\delta$ *versus* ^{1}H distance from the porphyrin plane [17] for all non-equivalent protons in both **1a** and **1b** components of **1**.(Ru(CO)TPP)$_2$ shows an excellent correlation for protons labelled α–δ (Figure 2). The rigid nature of **1a**, allowing it to act as a "molecular ruler", combined with the linear nature of this correlation becomes useful in providing structural information concerning the relative positions of the probe nucleii (and hence the NDI units) with respect to the porphyrin ring system for the more flexible **1b** in **1**·(Ru(CO)TPP)$_2$ [18, 19]. On the time-scale of the 300 MHz ^{1}H NMR experiments, the average chemical shift differences ($\Delta\delta$) of the probe protons ε in **1b**·(Ru(CO)TPP)$_2$ (**1b** = **1a** = −0.15 p.p.m.) correlate with the expected conformational freedom of the NDI around the ethylene spacer in **1b**. This $\Delta\delta$ is consistent with a time-averaged distance of ca. 9 Å from the porphyrin plane, as opposed to the 11.5 Å distance an extended conformation would afford.

Steady-state fluorescence spectra recorded upon titration of CH_2Cl_2 solutions of either **1a** or **1b** to Zn(II)TTP show significant quenching of the porphyrin fluorescence, consistent with a photo-induced ET process between the donor and acceptor components. The excitation wavelength chosen for fluorescence experiments (604 nm) avoids excitation of the NDI, while favouring excitation of complexed rather than free Zn(II)TTP. Energy transfer from photo-excited Zn(II)TTP to NDI is precluded as a possible quenching mechanism as the excited singlet energy of NDI is higher than that of Zn(II)TTP. Fluorescence decay profiles, recorded using the time-correlated single-photon counting technique [20], confirm that the excited state lifetime (τ) of the porphyrin is reduced when complexed to NDI. The fluorescence of Zn(II)TTP alone in deaerated CH_2Cl_2 decayed exponentially with a lifetime of 1.77 ns (τ_0). Upon addition of NDI the fluorescence decay was bi-phasic, a 1.77 ns component (due to uncomplexed Zn(II)TTP) and a short-lived component (τ_c) attributed to complexed Zn(II)TTP undergoing photoinduced ET. The relative contributions of the two lifetime components change with concentration reflecting the extent of complexation. For **1b**·ZnTTP, τ_c was found to be 0.29 ns, while for **1a**·ZnTTP, τ_c was of the order of the time-resolution of the detection system employed and can be given an upper limit of 0.10 ns. These lifetimes indicate fluorescence quenching of 84% and >94% for Zn(II)TTP complexed to **1b** and **1a**, respectively (Figure 3).

The quenched fluorescence lifetimes correspond to rates of ET from Zn(II)TTP to NDI of $2.88\times10^9\ s^{-1}$ for **1b**·ZnTTP, and $>9.44\times10^9\ s^{-1}$ for **1a**·ZnTTP consistent with the recent findings of Flamigni for **1a** in a bis-porphyrininc host [6d]. Assuming that the same orientation effects occur in both the ruthenium and zinc analogues, the slower ET rate in **1b** indicates that extending the pyridyl linker can attenuate the electronic coupling between donor and acceptor compared to **1a**.

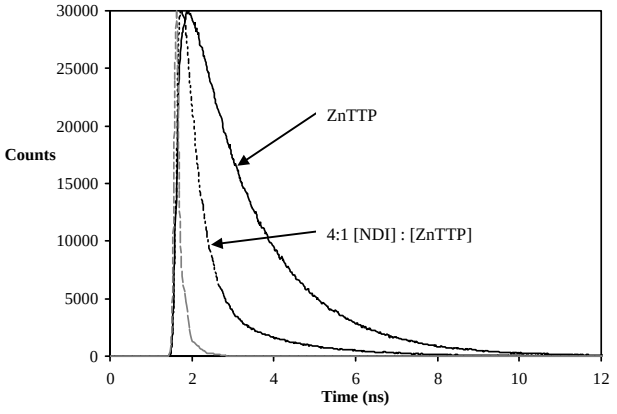

Figure 3. Fluorescence decay profiles obtained in deaerated CH_2Cl_2 (λ_{ex} = 604 nm) showing the quenching of ZnTPP fluorescence upon addition of a fourfold excess of **1b**. Grey profile = instrument response.

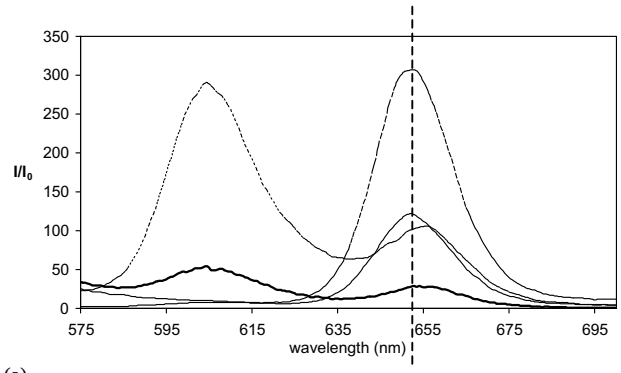

(a)

(b)

Input		Output
x	y	F_{650}
0	0	1
0	1	1
1	0	1
1	1	0

Figure 4. (a) Changes in the emission spectrum upon the addition of $Zn(OAc)_2{\cdot}2H_2O$, **1b**, or a mix of $Zn(OAc)_2{\cdot}2H_2O$ and **1b** to $TTPH_2$ in CH_2Cl_2 ($\lambda_{ex} = 400$ nm). (b) The truth table demonstrates a NAND function at 650 nm.

This provides an excellent means of tuning the rate of ET occurring in this simple bichromophoric system.

The wealth of spectroscopic change upon metallation, complexation and excitation observed in the formation and operation of **1b**·ZnTTP as a transduction device was then investigated with reference to $TTPH_2$ acting as an optical logic gate. Monitoring the fluorescence at 650 nm upon the addition of **1b**, Zn^{2+} and a mix of **1b** and Zn^{2+} yields a truth table (Figure 4) that leads to a NAND function. The NAND function [21, 22] is the complement of the AND function [23] and results in 0 only with the addition of the two inputs. In the case of **1b**·ZnTTP, this result arises through the photoinduced electron transfer step that occurs upon ligation. The importance of the NAND gate in standard electronic logic systems is mainly because it is easily constructed with transistor circuits and because Boolean functions can be implemented with them [24].

Conclusions

In conclusion we have shown that efficient ET transfer can occur across a simple bichromophoric system held together by Zn···N interactions and that the bridging unit provides a means of tuning the rate of ET in such systems. The spectroscopic differences between free-base, metallated and axially ligated porphyrins might also provide a plausible approach to the generation of molecular logic devices that operate optically as evinced by the generation of a NAND gate. We have further demonstrated a correlation between the distance from the porphyrin ring and the change in chemical shift ($\Delta\delta$), which might provide useful for the determination of orientations in other porphyrinic systems. We are now using this knowledge in the generation of more complex metalloporphyrin assemblies that act in a combinational fashion to generate more complex logic operations.

Acknowledgements

This work was supported by the Australian Research Council through the Discovery scheme and the S.R.C for Green Chemistry (scholarship to M.A.P. Lee). J.A. Hutchison acknowledges an Australian Postgraduate Award. Technical assistance from Karl Bezak is also acknowledged.

Appendix A

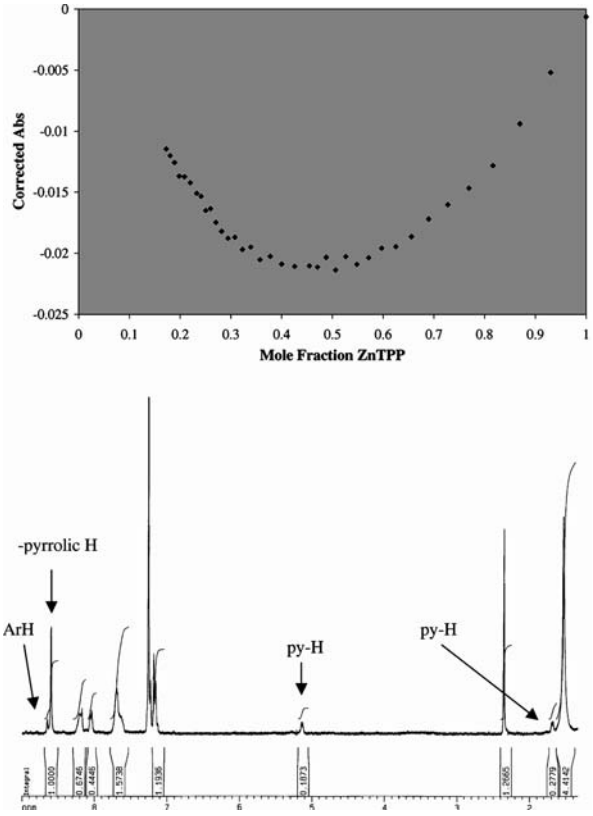

Figure A1. A Job's plot analysis [11] obtained in CH_2Cl_2 at 548 nm for the addition of **1b** to ZnTPP.

References

1. A.K. Burrell, D.L. Officer, P.G. Plieger, and D.C.W. Reid: *Chem. Rev.* **101**, 2751 (2001).
2. Y. Tong, D.G. Hamilton, J.-C. Meillon, and J.K.M. Sanders: *Org. Lett.* **1**, 1343 (1999).
3. B.J. Holliday and C.A. Mirkin: *Angew. Chem. Int. Ed.* **40**, 2022 (2001).

4. (a) C.C. Mak, N. Bampos, S.L. Darling, M. Montalti, L. Prodi, and J.K.M. Sanders: *J. Org. Chem.* **66**, 4476 (2001); (b) E. Stulz, C.C. Mak, and J.K.M. Sanders: *J. Chem. Soc.*, Dalton Trans. **5**, 604 (2001).
5. L. Giribabu, T.A. Rao, and B.G. Maiya: *Inorg. Chem.* **38**, 4971 (1999).
6. For examples of porphyrin-diimide systems see: (a) M.J. Gunter, N. Bampos, K.D. Johnstone, and J.K.M. Sanders: *New. J. Chem.* **25**, 166 (2001); (b) H.L. Anderson, C.A. Hunter, and J.K.M. Sanders: *J. Chem. Soc. Chem. Commun.* 226 (1989); (c) J.A. Cowan, J.K.M. Sanders, G.S. Beddard, and R.J. Harrison: *J. Chem. Soc. Chem. Commun.* 55 (1987); (d) H. Shiratori, T. Ohno, K. Nozaki, I. Yamazaki, Y. Nishimura, and A. Osuka: *J. Org. Chem.* **65**, 8747 (2000).
7. A number of examples of electron transfer in simple diads formed by self-assembly using metalloporphyrin coordination have appeared in the literature: (a) C.A. Hunter, J.K.M. Sanders, G.S. Beddard, and S. Evans: *J. Chem. Soc. Chem. Commun.* 1765 (1989); (b) F. D'Souza, G.R. Deviprasad, M.E. Zander, M.E. El-Khouly, M. Fujitsuka, and O. Ito: *J. Phys. Chem. B.* **106**, 4952 (2002); (c) L. Flamigni and M.R. Johnston: *New. J. Chem.* **25**, 1368 (2001).
8. C.J. Zhong, W.S.V. Kwan, and L.L. Miller: *Chem. Mater.* **4**, 1423 (1992).
9. G. Magnus and R. Levine: *J. Am. Chem. Soc.* **78**, 4127 (1956).
10. S.J. Langford, M.A.P. Lee, K.J. Macfarlane, and J.A. Weigold: *J. Incl. Phenom.* **41**, 135 (2001).
11. M. Nappa and J.S. Valentine: *J. Am. Chem. Soc.* **100**, 5075 (1978).
12. F.J.C. Rossotti and H. Rossotti: *The Determination of Stability Constants*, McGraw-Hill, New York (1961).
13. K.M. Kadish, L.R. Shiue, R.K. Rhodes, and L.A. Bottomley: *Inorg. Chem.* **20**, 1274 (1981).
14. Z.D. Hill and P. MacCarthy: *J. Chem. Educ.* **63**, 162 (1986).
15. B.G. Maiya, N. Bampos, A.A. Kumar, N. Feeder, and J.K.M. Sanders: *New J. Chem.* **25**, 801 (2001).
16. G.D. Fallon, S.J. Langford, M.A.P. Lee, and E. Lygris: *Inorg. Chem. Commun.* **5**, 715 (2002).
17. Because of the lack of structural information by X-ray crystallography, molecular modelling (Insight II) has been used as a suitable approximation to determine the distances between hydrogen atoms to the porphyrin plane. Ru–N distances were taken from published X-ray crystal structure data, see: K. Funatsu, A. Kimura, T. Imamura, A. Ichimura, and Y. Sasaki: *Inorg. Chem.* **36**, 1625 (1997).
18. E. Steiner and P.W. Fowler: *Chem. Phys. Lett.* **364**, 259 (2002).
19. K. Cross and M.J. Crossley: *Aust. J. Chem.* **45**, 991 (1992).
20. D.V. O'Connor and D. Phillips: *Time-Correlated Single Photon Counting*, Academic, London (1984).
21. D. Parker and J.A.G. Williams: *Chem. Commun.* 245 (1998).
22. V. Balzani, M. Venturi, and A. Credi: *Molecular Devices and Machines – A Journey into the Nanoworld*, Wiley-VCH, Weinheim (2003) chapter 9.
23. (a) A.P. de Silva and N.D. McClenaghan: *Chem. Eur. J.* **8**, 4935 (2002); (b) H. Xu, X. Xu, R. Dabestani, G.M. Brown, L. Fan, S. Patton, and H. Ji: *J. Chem. Soc.*, Perkin Trans. **2**, 636 (2002). (c) M.N. Stojanovic, T.E. Mitchell, and D. Stefanovic: *J. Am. Chem. Soc.* **124**, 3555 (2002); (d) A.P. de Silva, H.Q.N. Gunaratne, and C.P. McCoy: *Nature* **364**, 42 (1997).
24. M.M. Mano: *Digital Design*, Prentice Hall, New Jersey, 2nd edn. (1991).